# XMM-Newton Observations
# of the Southwestern Region of the Cygnus Loop

**Hiroyuki UCHIDA,  Hiroshi TSUNEMI, Satoru KATSUDA, Masashi Kimura (Osaka Univ.)**

**E-mail : uchida@ess.sci.osaka-u.ac.jp**

We observed the southwestern region of the Cygnus Loop in two pointings with XMM-Newton. The region observed is called "blow-up" region that is extended further in the south. The origin of the "blow-up" is not well understood while it is suggested that there is an another supernova remnant here in radio observation. To investigate the radial structure of this region in X-ray, we divided our fields of view into annular sectors. The spectra are well fitted by a two-component nonequilibrium ionization model. Judging from metal abundances obtained, it is consistent that the X-ray emission is the Cygnus Loop origin and we concluded that high-kTe component (~0.4keV) originates from the ejecta while low-kTe component (~0.2keV) is derived from the swept-up interstellar medium. The flux of low-kTe component is much less than that of high kTe component, suggesting the ISM component is very thin. Also, the relative abundances in the ejecta component shows similar values to those obtained from previous observations of the Cygnus Loop. These facts strongly support the idea that the nature of the "blow-up" region is the shock breakout of the Cygnus Loop itself rather than the extra supernova remnant. From the ejecta component, we calculated the masses for various metals and estimated the mass of the progenitor star to be 12-20 solar mass.

## 1. XMM-Newton Observations
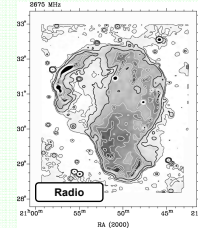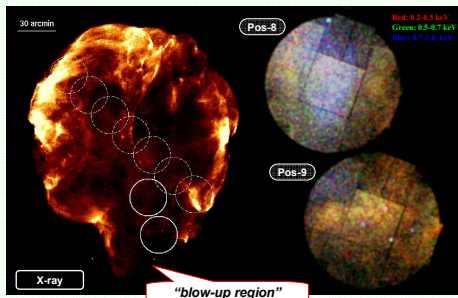


Fig.1: Left, ROSAT HRI image of the entire Cygnus Loop. Right, The three colored image of the Pos-8 and 9 with XMM-Newton.

Fig.2: The intensity map of the entire Cygnus Loop at 2675 MHz as observed with the Effelsberg 100m telescope[5].

The Cygnus Loop is one of the brightest Supernova Remnant (SNR) in the X-ray sky. The age is estimated to be ~10,000 yr. Since the distance is comparatively close to us (540 pc)[1], the apparent size is quite large (2.5° × 3.5°)[2], which enables us to study the plasma structure of the Loop. Figure 1 left shows the ROSAT HRI image of the entire Cygnus Loop. Tsunemi et al. observed Cygnus Loop along the diameter from the northeast to the southwest (named Pos1-7, the dotted circles represent the FOV) with XMM-Newton and studied the radial plasma structure[3]. They showed that the major part of the FOV requires a two-component kTe model. The results indicate that the abundances of the ejecta component are relatively high and each element is nonuniformly distributed: Si, S and Fe are concentrated in the inner region. They also estimated the progenitor star's mass to be 15 solar mass.

Although the Cygnus Loop is almost circular in shape, we can see some breakout in the southwest. It is called the "blow-up" region. The origin of the "blow-up" is not well understood. Aschenbach & Leahy have explained this extended structure as a breakout into a lower density ISM[4]. On the other hand, Uyaniker et al. suggested the existence of a secondary SNR in the southwest from a radio observation[5](see figure 2). Our observations were performed in a direction from the Cygnus Loop center toward the south "blow-up" region. Fig. 1 right shows the three colored image of the FOV. We call the north observation for Position-8 (Pos-8) and the south observation for Position-9 (Pos-9), respectively. The effective exposure time was 3.5ks (Pos-8) and 6.4ks (Pos-9), respectively. Both observations were performed on May 13 2006, during the XMM-Newton A-5 observing cycle.

## 2. Spatially Resolved Spectral Analysis
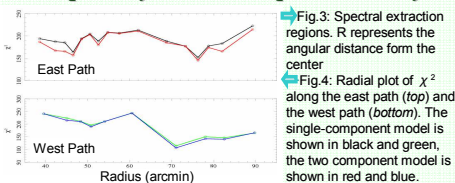


Fig.3: Spectral extraction regions. R represents the angular distance form the center

Fig.4: Radial plot of $\chi^2$ along the east path (*top*) and the west path (*bottom*). The single-component model is shown in black and green, the two component model is shown in red and blue.

To investigate the plasma structure of Pos-8 and 9, we divided our FOV into two paths: the east and west path, and, moreover, divided several annular regions as shown in figure 3. We set the annular center on the nominal center of the Loop. In order to equalize the statistics, we determined the annular widths such that each region has at least 5,000 photons. In this way, we have 26 annular sectors. We extracted the spectrum and fitted with the single-kTe and two-kTe nonequilibrium ionization (NEI) model.

Figure 4 shows the comparison of the $\chi^2$ values between the single component model and the two component model. From fig. 4, we found that the additional component is not so required in most regions. Figure 6 shows an example spectrum from the sector at R=42.5' (R represents the angular distance form the center) where the $\chi^2$ values were significantly improved by using the two component model. Top and bottom panels show the fit results of single-kTe model and two-kTe model, respectively. Even in this region, the contribution of the additional low-kTe component is not so large. It suggests that the ISM component is very thin almost everywhere in Pos-8 and 9.
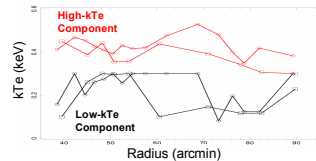


Fig.5: Temperature distributions of the two components as a function of radius. Circles and squares show the east path and the west path, respectively.

Fig.6: An example spectrum at R=42.5'. Top and bottom panels show the best-fit curves with the single-kTe NEI model and the two-kTe model, respectively.



single-kTe NEI model

$X^2$ / dof = 187 / 133

two-kTe NEI model

high-kTe Component

Low-kTe Component

$X^2$ / dof = 167 / 130

## 3. Abundance Ratios of Heavy Elements

From the spectral analysis, we find that the thickness of the shell is thin in Pos-8 and 9. This means that the X-ray emission mainly comes from the ejecta component in this region. Then we calculated the abundances of ejecta component for various elements from the fitting parameters of the high-kTe component.

Figure 7 shows the abundance ratios of heavy elements (Ne, Mg, Si [=S], Fe [=Ni]) relative to O of the high-kTe component. At the bottom right panel, these values are plotted on the same coordinate. It is said that the abundance ratios of Si, Fe are relatively high compared to those of Ne, Mg. This tendency is not changed in our observing region and consistent with the other Cygnus Loop observation such as Tunemi et al. (2007).



Fig.7: Abundance ratios of heavy elements (Ne, Mg, Si[=S], Fe[=Ni]) relative to O of the high-kTe component. Circles and squares show the east path and the west path, respectively. At the bottom right panel, these values are plotted on the same coordinate.
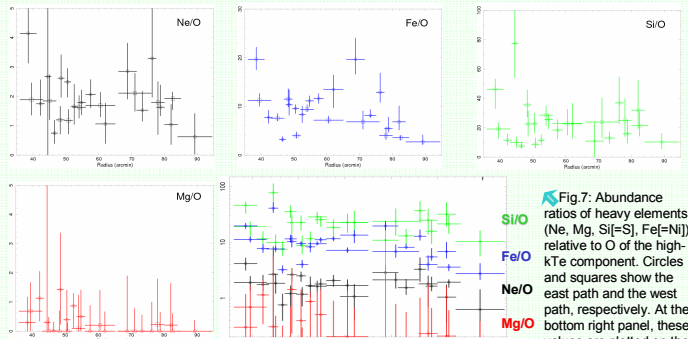
## 4. Emission Measures of Heavy Elements

We also measured the Emission Measures ( $EM = \int n_e n_H dl [cm^{-5}]$ ) of various heavy elements in the ejecta such as O [=C=N], Ne, Mg, Si [=S], Fe [=Ni] .

Figure 8 shows the EM distribution for these elements as a function of radius. These results show the tendency to decrease the EM from the inner region to the outer region, which is particularly prominent for the distribution of Fe. Under the assumption of the uniform density, it is reasonable to consider that the high-kTe component is ejecta origin and that these distributions are reflected in the spherical structure of the Cygnus Loop.
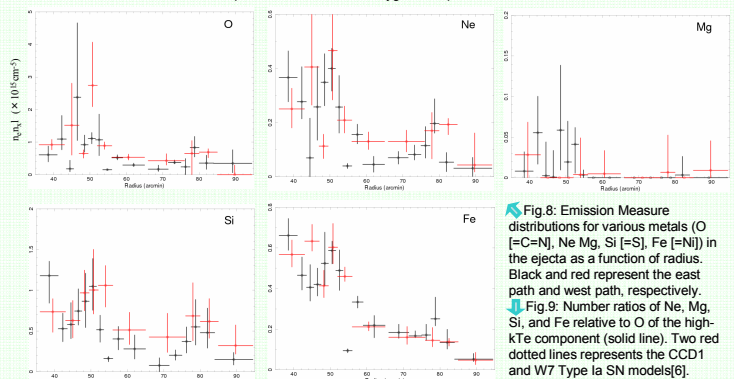


Fig.8: Emission Measure distributions for various metals (O [=C=N], Ne Mg, Si [=S], Fe [=Ni]) in the ejecta as a function of radius. Black and red represent the east path and west path, respectively.

Fig.9: Number ratios of Ne, Mg, Si, and Fe relative to O of the high-kTe component (solid line). Two red dotted lines represents the CCD1 and W7 Type Ia SN models[6]. Dotted blue, light blue, magenta, green lines represent core-collapse models with progenitor masses of 12, 13, 15, 20 solar, respectively[7].

## 5. Discussion and Conclusion

We observed the southwest region of the Cygnus Loop with XMM-Newton. To examine the radial plasma structure, we divided our FOV into 26 annular sectors and fitted the spectrum extracted from each region with two-kTe NEI model. From the spectral analysis, we found that the emission from the low-kTe component is relatively low which suggests that the thickness of the shell is thin in Pos-8 and 9. Previous study of Pos1-7 have showed the same tendency in the southwest and our result confirmed it. Therefore, we suggest that the nature of the "blow-up" region is the shock breakout of the Cygnus Loop rather than the extra SNR. We also calculated the abundance ratio and EM for various metals from the high-kTe component and showed that the abundance ratios of Si and Fe are relatively high compared to those of Ne and Mg. The EMs of metals (particularly Fe) decrease toward the outer region of the loop.

From these results, it is reasonable to consider that the emission of the high-kTe component originates from the ejecta of the Cygnus Loop. If the secondary SNR exists in southwest, the contribution of the X-ray emission to the spectra is less than that of the Cygnus Loop. Therefore, we can estimate the mass of the progenitor star of the Cygnus Loop from the EM of the high-kTe component. Figure 9 shows the number ratios of Ne, Mg, Si and Fe relative to O of the ejecta component. The relation of each element is closer to the core-collapse models than the Type Ia SN models. From fig. 9, we estimate the progenitor mass to be 12-20 solar mass. The number ratios of Si and Fe are higher than any core-collapse models, which is similar to the result of the Pos1-7 observation. Tsunemi et al. reported that Si and Fe were more abundant in the southwest than the northeast. These results implies an asymmetric explosion of the progenitor star.

## References

[1] Blair, W. P., Sankrit, R., & Raymond, J. C., 2005, AJ, 129, 2268
[2] Levenson, N. A., Graham, J. R., & Walters, J. L., et al. 1997, ApJ, 484, 304
[3] Tsunemi, H., Katsuda, S., Nemes, N. & Miller, E. D. 2007, ApJ 671,1717
[4] Aschenbach, B., & Leahy, D. A. 1999, A&A, 341, 602

[5] Uyaniker, B., Reich, W., Yar, A., & Fürst, E. 2004, A&A, 426, 426, 909
[6] Iwamoto, K., Brachwitz, F., Nomoto, K., et al. 1999 ApJS, 125, 439
[7] Woosley, S. E., & Weaver, T. A. 1995, ApJS, 101, 181
[8] Miyata, E, Katsuda, S., Tsunemi, H., et al. 2006, PASJ, 59, S163
[9] Hatsukade, I. & Tsunemi, H. 1990, ApJ, 362, 566
[10] Sun X., Reich, W., Han, J. L., Reich, P., et al. 2006 A&A, 447, 937

[11] Miyata, E., & Tsunemi, H. 1999, ApJ, 525, 305
[12] Katsuda, S., Tsunemi, H., Uchida, H., et al. 2008, PASJ 60, SP1, S115
[13] Katsuda, S., Tsunemi, H., Miyata, E., Mori, K., et al. 2008, PASJ 60, S107
[14] Uyaniker, B., Reich, W., Yar, A., Kothes, R Fürst, E. 2002, A&A, 389, L61
[15] Anders, E., & Greevesse, N. 1989, Geochim. Cosmochim. Acta, 53, 197
[16] Hester, J. J., Raymond, J. C. & Blair, W. P. 1994, ApJ, 420, 721